

MDA5-autoimmunity and Interstitial Pneumonitis Contemporaneous with the COVID-19 Pandemic (MIP-C)

Authors

Khizer Iqbal*¹, Saptarshi Sinha*², Paula David*¹, Gabriele De Marco^{3, 4, 5}, Sahar Taheri⁶, Ella McLaren², Sheetal Maisuria⁴, Gururaj Arumugakani^{7, 8}, Zoe Ash⁹, Catrin Buckley¹, Lauren Coles¹, Chamila Hettiarachchi³, Gayle Smithson³, Maria Slade³, Rahul Shah¹, Helena Marzo-Ortega⁴, Mansoor Keen⁹, Catherine Lawson¹⁰, Joanna Mclorinan¹, Sharmin Nizam³, Hanu Reddy¹¹, Omer Sharif¹², Shabina Sultan¹¹, Gui Tran¹⁰, Mark Wood¹, Samuel Wood¹, Pradipta Ghosh^{2, 13‡}, Dennis McGonagle^{1,4‡}

*These authors contributed Equally as first author

Affiliations

¹Leeds Teaching Hospitals NHS Trust, Rheumatology Department, Leeds, United Kingdom. ²Department of Cellular and Molecular Medicine, School of Medicine, University of California San Diego, La Jolla, CA, 92093, USA. ³Mid Yorkshire Teaching NHS Trust, Rheumatology, Wakefield, United Kingdom ⁴University of Leeds, Leeds Institute of Rheumatic and Musculoskeletal Medicine, Leeds, United Kingdom. ⁵NIHR Leeds Biomedical Research Centre, Leeds Teaching Hospitals NHS Trust, Leeds, United Kingdom. ⁶ Department of Computer Science and Engineering, Jacob's School of Engineering, University of California San Diego, La Jolla, CA. 92093, USA. ⁷Leeds Teaching Hospitals NHS Trust, Pathology, Leeds, United Kingdom, ⁸University of Leeds, Immunology, Leeds, United Kingdom. ⁹Bradford Teaching Hospitals NHS Foundation Trust, Rheumatology, Bradford, United Kingdom. ¹⁰Harrogate and District NHS Foundation Trust, Rheumatology, Harrogate, United Kingdom. ¹¹Airedale NHS Foundation Trust, Rheumatology, Steeton with Eastburn, United Kingdom. ¹²Calderdale and Huddersfield NHS Foundation Trust, Rheumatology, Huddersfield and Halifax, United Kingdom. ¹³Department of Medicine, School of Medicine, and Veterans Affairs Medical Center, University of University of California San Diego, La Jolla, CA. 92093, USA.

‡Corresponding Authors:

Dennis McGonagle PhD FRCPI

Leeds Teaching Hospitals NHS Trust, Rheumatology Department, Leeds, United Kingdom | University of Leeds, Leeds Institute of Rheumatic and Musculoskeletal Medicine, Leeds, United Kingdom |

Email: d.g.mcgonagle@leeds.ac.uk

Pradipta Ghosh, M.D.

Professor, Departments of Medicine and Cellular and Molecular Medicine, University of California San Diego; 9500 Gilman Drive (MC 0651), George E. Palade Bldg, Rm 232, 239; La Jolla, CA 92093, USA | Phone: 858-822-7633 | Email: prghosh@ucsd.edu

40 Abstract

41 **Background:** Anti-MDA5 (Melanoma differentiation-associated protein-5) positive dermatomyositis
42 (MDA5⁺-DM) is characterised by rapidly progressive interstitial lung disease (ILD) and high mortality.
43 MDA5 senses single-stranded RNA and is a key pattern recognition receptor for the SARS-CoV-2 virus.

44 **Methods:** This is a retrospective observational study of a surge in MDA5 autoimmunity, as determined
45 using a 15 muscle-specific autoantibodies (MSAs) panel, between January 2018-December 2022 in
46 Yorkshire, UK. MDA5-positivity was correlated with clinical features and outcome, and regional SARS-
47 CoV-2 positivity and vaccination rates. Gene expression patterns in COVID-19 were compared with
48 autoimmune lung disease and idiopathic pulmonary fibrosis (IPF) to gain clues into the genesis of the
49 observed MDA5⁺-DM outbreak.

50 **Results:** Sixty new anti-MDA5⁺, but not other MSAs surged between 2020-2022, increasing from 0.4%
51 in 2019 to 2.1% (2020), 4.8% (2021) and 1.7% (2022). Few (8/60) had a prior history of confirmed
52 COVID-19, peak rates overlapped with regional SARS-COV-2 community positivity rates in 2021, and
53 58% (35/60) had received anti-SARS-CoV-2 RNA vaccines. Few (8/60) had a prior history of COVID-19,
54 whereas 58% (35/60) had received anti-SARS-CoV-2 RNA vaccines. 25/60 cases developed ILD which
55 rapidly progression with death in 8 cases. Among the 35/60 non-ILD cases, 14 had myositis, 17
56 Raynaud phenomena and 10 had dermatomyositis spectrum rashes. Transcriptomic studies showed
57 strong *IFIH1* (gene encoding for MDA5) induction in COVID-19 and autoimmune-ILD, but not IPF, and
58 *IFIH1* strongly correlated with an IL-15-centric type-1 interferon response and an activated CD8⁺ T cell
59 signature that is an immunologic hallmark of progressive ILD in the setting of systemic autoimmune
60 rheumatic diseases. The *IFIH1* rs1990760TT variant blunted such response.

61 **Conclusions:** A distinct pattern of MDA5-autoimmunity cases surged contemporaneously with
62 circulation of the SARS-COV-2 virus during COVID-19. Bioinformatic insights suggest a shared
63 immunopathology with known autoimmune lung disease mechanisms.

64 Introduction

65 Dermatomyositis (DM) is a systemic autoimmune disease characterized by muscle and skin
66 inflammation and potentially fatal- internal organ involvement, typically interstitial lung disease (ILD)
67 leading to progressive pulmonary fibrosis. The first autoantibody defined in DM was anti-Jo-1, which
68 targets the enzyme histidyl-tRNA synthetase. Since then, many muscle-specific autoantibodies (MSA)
69 emerged, often linked to different clinical phenotype patterns and different MHC-II associations that
70 further underpin the veracity of the autoimmunity concept in DM ¹⁻⁴.

71 One of the well-recognised clinical phenotype of DM is clinically amyopathic dermatomyositis (CADM)
72 that is associated with rapidly progressive ILD and is attributed to the Retinoic acid-inducible gene 1
73 (RIG-1)-like receptor family gene, *IFIH1*, which encodes the protein Melanoma differentiation-
74 associated protein-5 (MDA5) ⁵. Most MDA5+ cases predating the COVID-19 pandemic reported
75 significant ILD but a relative lack of myositis or the classical DM heliotropic rash; instead, they showed
76 cutaneous phenotypes including skin ulceration and tender palmar papules ⁶.

77 Here we report a surge in the rate of anti-MDA5 positivity testing in our region (Yorkshire) in the
78 second year of the COVID-19 pandemic, which was notable because this entity is relatively rare in the
79 UK. This was intriguing because MDA5 is a RIG-1 helicase ⁷ tasked to sense single-stranded RNA and is
80 a key pattern recognition receptor for the contemporary SARS-CoV-2 virus ⁸. Variants of the MDA5
81 protein-coding gene, *IFIH1* (rs1990760 TT) have recently been shown to confer protection in COVID-
82 19 infections and experienced better outcomes ⁹.

83 In this retrospective study, we explored the phenotypes and epidemiological factors associated with
84 the cluster of MDA5⁺-related disease at our centre which provides autoantibody testing for a 3.6
85 million-large population ([Figure 1-Steps 1-2](#)). We describe this phenomenon as MDA5 autoimmunity
86 with interstitial pneumonitis cotermporaneous with the CCOVID-19 pandemic (MIP-C) that reflects the
87 different epidemiology and clinical patterns reported herein compared to previously defined MDA5
88 related autoimmunity. We also leveraged transcriptomic datasets to explore putative mechanisms of
89 this emergent MDA5-associated disease in the setting of SARS-CoV-2 infection ([Figure 1-Step 3](#)).
90 Specifically, as post COVID pneumonia is associated with pulmonary fibrosis, we leveraged datasets to
91 compare acute COVID-19 lung disease, autoimmune lung disease and idiopathic pulmonary fibrosis
92 (IPF) to gain clues into the genesis of the observed MDA5⁺-DM outbreak. Finally, we presented a
93 working model that links severity of anti-viral cytokine response to *IFIH1* induction and genetics and
94 ultimately, to the distinct immunophenotype specific for MSA-associated progressive ILD ([Figure 1-
95 Step 4](#)). These findings provide insights into the observed surge in anti-MDA5 positivity during the

96 COVID-19 pandemic and the potential role of RNA viruses in rapidly progressive ILD and other
97 autoimmune conditions.

98

99 Methods

100 Study design

101 The Leeds Teaching Hospitals NHS Trust serves as an immunology laboratory reference for the wider
102 Yorkshire region of the UK. We audited the increased anti-MDA5 positivity in relationship to other
103 MSA (Euroimmun immunoblot©) that included MDA5⁺ cases. This was based on both increased rate
104 of anti-MDA5 related immunology reporting and multiple physicians seeing MDA5 related disease for
105 the first time, combined with emergent literature reporting COVID-19 era anti-MDA5-related disease
106 ^{1-4,10-28}. We collected data on the number of MDA5+ tests per year between January 2018 to December
107 2022. The clinical notes review focused on patterns of symptomatic MDA5 disease (including degree
108 of ILD); muscle or other organs involvement, therapy, therapy responses and survival data.

109 We also leveraged Public Health England (PHE) data on SARS-CoV-2 monthly positivity rates in the
110 Yorkshire region. We also evaluated data on lung involvement and concomitant SARS-CoV-2 infection,
111 recent SARS-CoV-2 infection or recent SARS-CoV-2 vaccination or both infection and vaccination by
112 searching for confirmed PCR positivity for infection or confirmation of vaccination status including
113 number of vaccines administered as gleaned from “NHS spine” system, a system that supports the IT
114 infrastructure for health and social care for England, joining together over 44,000 healthcare systems
115 in 26,000 organizations ²⁹.

116 Ethics Statement

117 Ethics committee/ Institutional Research Board (IRB) of University of Leeds, UK, waived ethical
118 approval for this work. This study was reported according to the “CAse REports” (CARE) guidelines
119 [<https://www.care-statement.org/>]. All participants recruited granted verbal or written consent to the
120 local treating physicians for the use of their anonymized data. An approved retrospective audit of
121 service delivery at our institution, and a formal IRB approval was not needed.

122 Computational Analyses

123 *Transcriptomic Datasets and Data Analyses:* To explore potential mechanistic links between COVID
124 infection and lung disease we analyzed several publicly available datasets (COVID-19, n = 240; ILD, n =
125 316; viral pneumonitis, n = 1038), a complete catalog of which is presented in **Supplemental**
126 **Information 1**). To decipher which immunophenotype is induced in the setting of COVID-19,
127 previously validated lung or PBMC-based gene signatures from distinct lung diseases were used: (i)
128 idiopathic pulmonary fibrosis (IPF); (ii) hypersensitivity pneumonitis (HP); (iii) systemic autoimmune

129 rheumatoid diseases (SARDs) such as systemic sclerosis and MDA5⁺-DM; and (iv) well-defined
130 signatures of so called “AT2 cytopathies”, i.e., ER stress, stem cell dysfunction, senescence, and
131 telomere shortening, which have been implicated in driving fibrotic lung disease after diffuse alveolar
132 injury, as in the setting of severe COVID-19³⁰ and IPF³¹). All gene signatures used in this work are
133 presented in an excel sheet, alongside the original source articles (**Supplemental Information 2**).

134 *Single Cell RNA Sequencing Analysis*: Single Cell RNASeq data from GSE145926 was downloaded from
135 Gene Expression Omnibus (GEO) in the HDF5 Feature Barcode Matrix Format. The filtered barcode
136 data matrix was processed using Seurat v3 R package. B cells (CD19, MS4A1, CD79A), T cells (CD3D,
137 CD3E, CD3G), CD4 T cells (CCR7, CD4, IL7R, FOXP3, IL2RA), CD8 T cells (CD8A, CD8B), Natural killer cells
138 (KLRF1), Macrophages, Monocytes and DCs (TYROBP, FCER1G), Epithelial (SFTPA1, SFTPB, AGER,
139 AQP4, SFTPC, SCGB3A2, KRT5, CYP2F1, CCDC153, TPPP3) cells were identified using relevant gene
140 markers using SCINA algorithm.

141 Several publicly available microarrays and RNASeq databases were downloaded from the National
142 Center for Biotechnology Information (NCBI) Gene Expression Omnibus (GEO) server. Gene expression
143 summarization was performed by normalizing Affymetrix platforms by RMA (Robust Multichip
144 Average) and RNASeq platforms by computing TPM (Transcripts Per Millions) values whenever
145 normalized data were not available in GEO. We used log₂(TPM +1) as the final gene expression value
146 for analyses. GEO accession numbers are reported in figures and text. A catalog of all datasets analyzed
147 in this work can be found in **Supplemental Information 1**.

148 *Gene Expression Analyses*: The expression levels of all genes in these datasets were converted to
149 binary values (high or low) using the *StepMiner* algorithm^{32,33} which undergoes an adaptive regression
150 scheme to verify the best possible up and down steps based on sum-of-square errors. The steps are
151 placed between data points at the sharpest change between expression levels, which gives us the
152 information about threshold of the gene expression-switching event. To fit a step function, the
153 algorithm evaluates all possible steps for each position and computes the average of the values on
154 both sides of a step for the constant segments. An adaptive regression scheme is used that chooses
155 the step positions that minimize the square error with the fitted data. Finally, a regression test statistic
156 is computed as follows:

$$157 \quad F \text{ stat} = \frac{\sum_{i=1}^n (\hat{X}_i - \bar{X})^2 / (m - 1)}{\sum_{i=1}^n (X_i - \hat{X}_i)^2 / (n - m)}$$

158 Where X_i for $i = 1$ to n are the values, \hat{X}_i for $i = 1$ to n are fitted values. M is the degrees of freedom
159 used for the adaptive regression analysis. \bar{X} is the average of all the values:

160
$$\bar{X} = \frac{1}{n} * \sum_{j=1}^n X_j$$

161 For a step position at k , the fitted values \hat{X}_i are computed by using

162
$$\frac{1}{k} * \sum_{j=1}^n X_j$$

163 for $i = 1$ to k and

164
$$\frac{1}{(n - k)} * \sum_{j=k+1}^n X_j$$

165 for $i = k + 1$ to n .

166 Gene expression values were normalized according to a modified Z-score approach centered around
167 *StepMiner* threshold (formula = $(\text{expr} - \text{SThr})/3 * \text{stddev}$). The normalized expression values for every
168 genes were added together to create the final score for the gene signature. The samples were ordered
169 based on the final signature score. Classification of sample categories using this ordering is measured
170 by ROC-AUC (Receiver Operating Characteristics Area Under The Curve) values. Welch's Two Sample
171 t-test (unpaired, unequal variance (`equal_var=False`), and unequal sample size) parameters were used
172 to compare the differential signature score in different sample categories. Violin plots are created
173 using python seaborn package version 0.10.1. Differentially expressed genes are identified using
174 DESeq2 package in R.

175 *Correlation plot*: StepMiner normalized composite score of gene signatures were plotted against each
176 other for all the patients. For each two signatures, linear least-squares regression has been obtained
177 using SciPy LLS model (`scipy.stats.linregress`). R^2 and p-value for each pair of signatures are plotted as
178 heatmap using seaborn (`seaborn.heatmap`) package.

179 *Multivariate Analyses*: To assess which factor(s) may influence MDA5 induction upon exposure to
180 SARS-CoV2, multivariate regression has been performed on the bulk sequence COVID-19 PBMC
181 datasets (GSE233626 [updated with additional variables from GSE168400] and GSE233627 (updated
182 with additional variables from GSE177025). Multivariate analysis of GSE233626 models the degree of
183 *IFIH1* induction in samples (base variable) as a linear combination of gender, age, ventilation,
184 hypoxemia with/without genotype. Multivariate analysis of GSE233627 also models the degree of
185 *IFIH1* induction in samples (base variable) as a linear combination of the same variables as above, and
186 an additional variable- that of treatment with systemic corticosteroids. Here, the statsmodels module
187 from python has been used to perform Ordinary least-squares (OLS) regression analysis of each of the
188 variables. The choice of these datasets was driven by the criteria that they are high quality datasets

189 with maximal unique patient samples. The p-value for each term tests the null hypothesis that the
190 coefficient is equal to zero (no effect).

191 *Data and Code Availability:* All codes and datasets used in this work can be found at
192 https://github.com/sinha7290/COVID_mda5.

193 Results

194 **MDA5 positivity between 2018-2022.** Between January 2018 and December 2019, 6 new MDA5⁺
195 cases were identified, representing 1.2% and 0.4% MSA immunoblot positivity in the respective years
196 (**Figure 2A**). However, commencing in 2021, after the second UK SARS-CoV-2 infection wave, we noted
197 an increase in new MDA5⁺ cases (**Figure 2**). The total numbers of new cases were 9, 35 and 16 in 2020,
198 2021 and 2022 respectively (**Figure 2A**). Irrespective of the fact that MSA requisitions requests
199 approximately doubled during the same period of time, an increased rate of MDA5 positivity was
200 evident, rising from 1.2% in 2018 and 0.4% in 2019 to to 2.2% in 2020, 4.8% in 2021 and decreasing to
201 1.7% in 2022. The other MSAs did not exhibit this striking pattern of increase (**Figure 2A-top**).

202 **Clinical features of the 60 new MDA5 positive cases.** Thirty-two/60 were of white ethnic background
203 [either British or other still classified as white, according to 2021 UK census methodology³⁴]. Three/60
204 were of Asian/Asian British (all of these Indian/Pakistani) background; 2 were of Black Caribbean and
205 1 of Black African ethnic background and 4 were considered “any other ethnic group”. Four patient
206 was of other Asian background (not Chinese) with no ethnicity data for 14/60 patients.

207 All 60 patients experienced some features consistent with an autoimmune disease, their average age
208 was 56.17 years (median 56; standard deviation 19.9; absolute range 9-90; inter-quartile range 43.75-
209 71.25) and 36/60 (60%) were female. Of the 60 patients, 25 developed ILD with a mean age 60.28
210 years; median 66; standard deviation 18.56; absolute range 12-90; and inter-quartile range 51-73.
211 Twelve/25 (48%) were females. Almost half of this subgroup (12/25, 48%) rapidly progressed and 8 of
212 them died. By contrast, just 1 fatality was observed in the 35 patients who did not develop ILD (sepsis-
213 related). Out of 4 new paediatric patients in this series, none were fatal and none were vaccinated
214 against SARS-CoV2.

215 The 35 patient non-ILD group had a mean age of 53.23 years (median 54; standard deviation 20.6;
216 absolute range 9-89; inter-quartile range 40-69). 24/35 (68.6%) were females; 4/60 were < 18 years
217 old. Although the non-ILD subgroup was younger than their ILD counterparts (**Table 1**), this difference
218 was not statistically significant (Student T test p-value = 0.179). The two subgroups did not differ in
219 terms of gender representation (Fisher’s exact test p-value 0.120).

220 The main indication for requesting MSA testing in the ILD subgroup was dyspnoea with and without
221 associated myositic/DM features (**Table 1**, and **Supplemental Table 1**). The indication for performing
222 such testing in the non-ILD subgroup was cutaneous manifestations of DM or scleroderma-like clinical
223 features, as well as proximal myopathy (**Table 1** and **Supplemental Table 2**). There was one case of
224 confirmed myocarditis. The creatine kinase (CK) at baseline was available for 50/60 patients and its
225 average was 811.78 units per liter (U/L), however, the median was 90.5 U/L in keeping with CADM

226 phenotype (IQR 56.75-199); there was no statistically significant difference between ILD and non-ILD
227 groups (median 78 vs. 115, respectively Mann-whitney U test p value of 0.186). Of 35 non-ILD cases,
228 at least 9 (missing data on imaging for 9/35 patients) had muscle MRI, of them 5 were compatible with
229 myositis. Details of therapy are shown for each case in [Supplemental Tables 1-2](#).

230 **MDA5 positive ILD outcomes.** As expected the prognosis was poorer in the 25 patients in the ILD
231 patients. Chest CT was available in 24/25 cases, which demonstrated fibrosis and associated ground
232 glass changes in 6/25 cases; fibrotic changes only in 8/25 cases; ground glass changes only in 9/25
233 cases; ground glass changes with pneumomediastinum in 1 case. In keeping with the MDA5
234 phenotype, 8/25 patients progressed, most rapidly, and died despite intensive therapy; 4/25
235 developed progressive lung disease; 12/25 stabilised with or without specific therapy. There is one
236 patient with no available data regarding response to treatment. There was no evidence of myocarditis
237 in this subset and mortality was due to pulmonary disease ([Supplemental Table 1](#)). The only patient
238 of paediatric age in this group remains stable.

239 **Non-ILD MDA5 positive disease.** All MDA5⁺ cases had some clinical features of autoimmune
240 connective tissue disease, including cutaneous manifestations of DM or Raynaud's phenomenon
241 ([Table 1](#) and [Supplemental Table 2](#)). More patients in the non-ILD subgroup developed cutaneous
242 rash (10/35) and Raynaud's phenomenon (17/35), sometimes both, and proximal myopathy (14/35)
243 with only 1/35 developing "mechanic's hands" ([Supplemental Table 2](#)).

244 **Autoantibody testing.** There was no difference in ANA positivity between the ILD subgroup and the
245 the non ILD subgroup (60% positive in both groups, as determined by immunofluorescence). In both
246 subgroups SAE1 and Ro-52 were the auto-antibodies most often positive concomitantly to the anti-
247 MDA5. 15/25 patients in the ILD subgroup had additional MSA antibodies as compared to 21/35 in the
248 non-ILD subgroup (χ^2 test p-value = 0.930). 4/8 (50%) of patients who died in ILD subgroup had
249 additional MSA antibodies, being anti-small ubiquitin-like modifier-1 (SAE-1) MSA the most common,
250 evident in 3/4.

251 **Relationship to COVID-19 infection or vaccination.**

252 In lieu of patient autoimmune symptoms and signs, MDA5⁺ testing emerged only after the second
253 and third SARS-CoV-2 wave in the Yorkshire region ([Figure 2B](#)). Also, the highest rate of MDA5
254 positivity did occur during higher community SARS-COV-2 positivity during 2021 but the highest rate
255 of SARS-CoV-2 circulation was not followed by an immediate increased MDA5⁺ testing ([Figure 2B](#)).
256 8/60 had confirmed COVID-19 before anti-MDA-5⁺ test performed, and 7/60 were infected after the

257 diagnosis, with 2 of them flaring during the infection. Overall, 15/60 had confirmed SARS-CoV-2
258 infection with only 8/25 positive in the ILD subgroup and 7/35 in the non ILD subgroup.

259 As for vaccinations, the overall uptake of SARS-CoV-2 vaccination in the UK and Yorkshire region was
260 90% and we saw a strong overlap between vaccination timing in 2021 and the surge in MDA5+ disease
261 (Figure 2C) but such a close link with monthly confirmed infections was lacking (Figure 2B-C). 49/60
262 (81.6%) cases had documented evidence of SARS-CoV-2 vaccination; 20/25 in the ILD subgroup and
263 29/35 in non-ILD subgroup. 36/60 (60%) cases were vaccinated before anti-MDA5 positivity, 14/60
264 were vaccinated after, of which 2/14 had a disease flare. 11/60 (5/25 ILD and 6/35 non-ILD) were not
265 vaccinated at any point. In the ILD group, 14/25 (56%) were vaccinated preceding the MDA5+ test,
266 while in the nILD group 22/35 (62.9%) (χ^2 test p-value = 0.271).

267 Accordingly, most of the MDA5+ cases had either confirmed infection or confirmed SARS-CoV-2
268 vaccination. All the 4 patients of paediatric age, were not vaccinated (all of these developed MDA5
269 positivity after the pandemic started). Time-relationship to vaccine and infection for each individual
270 is summarized in Supplemental Tables 1-2.

271

272 COVID-19 lungs show induction of MDA5 (*IFIH1*) gene and signatures of SARD-related ILD

273 We leveraged available transcriptomic datasets to explore potential mechanisms of MDA5+ disease in
274 the setting of COVID-19. Analysis of bronchoalveolar lavage fluid from COVID-19 lungs by single cell
275 RNA sequencing (scSeq; Figure 3A) confirmed that *IFIH1* is induced significantly in diverse cells of the
276 lavage fluid (Figure 3B; arrow, bubble plot), alongside the robust induction of a set of several
277 previously validated signatures (Figure 3B):

- 278 (i) an intense IL-15-centric type 1 interferon (IFN) response, a.k.a, the *V*iral *P*andemic (ViP) and its
279 subset, severe(s)ViP signatures that was identified and rigorously validated using machine
280 learning (on ~45,000 samples) which capture the 'invariant' host response, i.e., the shared
281 fundamental nature of the host immune response induced by all viral pandemics, including
282 COVID-19³⁵;
- 283 (ii) a COVID-19 lung signature³⁶;
- 284 (iii) a set of 3 signatures indicative of alveolar type two (AT2) cytopathies in fibrotic lung disease,
285 i.e., (a) damage associated transient progenitor (DATP)³⁷, a distinct AT2 lineage that is a central
286 feature of idiopathic pulmonary fibrosis (IPF)³⁷⁻³⁹; (b) AT2-senescence signature⁴⁰; and (c)
287 Telomerase dysfunction signature, which was derived from aging telomerase knockout (Terc-
288 /-) mice⁴¹. Lung epithelial signatures of IPF were also induced (Figure 3B), most consistently in

289 the epithelium. However, gene signatures previously reported in ILDs that are related to
290 systemic autoimmune rheumatic diseases (SARDs), [which include systemic sclerosis (SSc), DM,
291 polymyositis (PM), rheumatoid arthritis (RA), primary Sjögren's syndrome] were induced in a
292 wide variety of cell types (Figure 3B).

293 When exosome vesicles isolated from the serum of COVID-19 patients during various phases
294 of the disease were applied to 2D cultures of lung or liver epithelial cells (see Figure 3C-D), *IFIH1* (see
295 Figure 3E-F; arrows) and gene signatures of AT2 cytopathies and autoimmune ILD were induced
296 significantly and specifically in the lung, but not liver cells. Consistent with its role as an innate immune
297 sensor of RNA viruses, the serum from the disease phase when viral RNA is detectable (S2 phase)
298 triggered a significant induction in *IFIH1* and autoimmune-ILD signature (but not IPF) (Figure 3C). We
299 conclude that both *IFIH1* and autoimmune-ILD signatures were induced *in vivo* and *in vitro* upon
300 exposure to viral RNA.

301

302 **Expression of MDA5 (*IFIH1*) gene and signatures of autoimmune ILD in COVID-19 PBMCs**

303 The observed induction of *IFIH1* in the immune cells within the lungs warranted a similar analysis of
304 peripheral blood mononuclear cells (PBMCs) from acute and convalescent COVID-19 subjects, using a
305 set of gene signatures that were previously validated in immune cells (enlisted in Figure 4A). We
306 prioritized a dataset that also included the information on the *IFIH1* genotype rs1990760 which has
307 recently been shown to impact the degree of inflammatory response and outcomes in COVID-19⁹.
308 *IFIH1* induction tightly and positively correlated with type 1 IFNs (Figure 4B; ViP), an *ISG15*⁺ CD8⁺
309 cytotoxic T-cell signature that was found to be associated with risk of progressive ILD in the setting of
310 MDA5 autoimmunity⁴² (Figure 4B; anti-MDA5-ILD) and a distinctive IFN response that is specific for
311 anti-MDA5+ DM (Figure 4B; anti-MDA5-DM IFNs). The rs1990760 TT variant that was found to be
312 protective, showed a clear pattern in each comparison tested; two clear groups were observed in each
313 comparison (Figure 4C).

314 Unlike autoimmune ILDs, the IPF-related ILDs are known to have a completely distinct
315 immunopathogenesis. We next leveraged a 52-gene PBMC-based IPF signature that was previously
316 discovered⁴³ and subsequently validated as a predictor of IPF progression in a prospective multicenter
317 study⁴⁴. The expression of *IFIH1* negatively correlated with the 52-gene PBMC-based IPF signature
318 (Figure 4B). Negative correlations were observed between *IFIH1* and another independent signature
319 for IPF (IPF-2; Figure 4D) and with a signature of hypersensitivity pneumonitis (HP; Figure 4D).

320 All these correlative patterns generally held true when rigorously tested across independent
321 PBMC datasets from diverse patient cohorts, representing COVID-19 (Figure 4E-F) and other viral
322 respiratory pandemics (Supplementary Figure 1). *IFIH1* induction consistently correlated with a type
323 1 IFN-centric immune response in MDA5 autoimmunity, but not with the immune response in IPF.

324

325 **Impact of severity, gender, steroids and *IFIH1* genotype on MDA5 (*IFIH1*) surge**

326 A subanalysis on the largest PBMC dataset that included information on gender and disease severity
327 revealed that *IFIH1*, anti-MDA5-ILD and ViP signatures were induced in less severe disease which did
328 not warrant ICU-level of care (Figure 4G), whereas the 52-gene risk signature for progressive IPF was
329 induced in more severe COVID-19 that required ICU care (Figure 4G); these observations held true in
330 both genders.

331 Next we created a multivariate model to decompose the covariance between the levels of
332 induction of *IFIH1* (base variable), genotype, gender, age, severity of ARDS; as determined using the
333 ratio of PaO₂/FiO₂) and the need for ventilation (Vent). The *IFIH1* rs1990760 genotype emerged as
334 the strongest determinant of the degree of induction of the *IFIH1*(MDA5) transcript (Figure 5A-left).
335 Age emerged as an independent variable when the rs1990760 TT variant was analyzed independently
336 (Figure 5A-middle); young age was associated with higher levels of induction of *IFIH1* transcripts.
337 Gender and the need for ventilation were covariates when the rs1990760 CT/CC variants were
338 analyzed independently (Figure 5A-right); female gender and moderate disease not requiring
339 ventilator support was associated with a higher level of *IFIH1* transcript surge.

340 A similar analysis on another independent dataset in which intervention was performed in the
341 form of systemic corticosteroid treatment. Such treatment is an independent protective factor
342 exclusively in the subjects with rs1990760 CT/CC variants, but not in those with the rs1990760 TT
343 variant (Figure 5B). Taken together, these findings reveal a complex interplay between *IFIH1* genotype
344 in which the rs1990760 TT variant offers age-dependent protection to the elderly. Among those who
345 lack this protective variant, female gender and less severe disease increases the degree of *IFIH1* surge,
346 whereas systemic therapy with steroids offers protection.

347

348 **The nature of the immunophenotype associated with the induction of MDA5 (*IFIH1*) transcript**

349 We asked if *IFIH1* induction may be associated with an age-dependent immunophenotype that
350 modulates the risk of progressive autoimmune ILD. We assessed the differentially expressed genes

351 (DEGs) between the two distinct groups of patients within the rs1990760 TT variant, i.e., low- and
352 high- inducers of the *IFIH1* transcript (Figure 5C-D). The *IFIH1*-high group induced 26 genes that are
353 enriched for type 1 IFN signals and cellular responses to the same (Figure 5E-F). Upregulated genes
354 are notable for markers of progressive autoimmune ILD, e.g., *CXCL10*⁴⁵, IFN-induced genes associated
355 with systemic autoimmune rheumatic diseases (SARD) [*IFI44L*, *LY6E*, *OAS3*, *RSAD2*⁴⁶], adaptive
356 immune hallmarks of MDA5+ DM [*IFI6*, *MX1*, *OAS2*⁴²] and *MX1*⁴⁷ (Figure 5F). These DEGs were
357 significantly induced in autoimmune ILD (Figure 5G; non-specific interstitial pneumonitis,
358 NSIP), compared to IPF (usual interstitial pneumonia, UIP). Similarly, when we analyzed the
359 DEGs in lung epithelial cells that were treated with acute vs convalescent serum derived
360 exosomes, we found that the Type 1-centric genes induced in the lung epithelium were
361 significantly induced also in NSIP compared to IPF (Supplementary Figure 2).

362 Discussion

363 Several COVID-19 era case reports or series of MDA5+ myositis or ILD have been reported in
364 the UK and internationally either in the setting of infection or post-vaccination^{1-4,10-28}. Our study is the
365 largest one to document the features and outcomes of this clinical syndrome, especially in 2021.
366 Approximately 42% of our MDA5+ cases have thus far had progressive ILD, with a third of these
367 proving fatal so far, in keeping with the known aggressive course of MDA5⁺-ILD^{48,49}.—Our clinical
368 epidemiologic observations, together with the transcriptomic analyses suggest that increased
369 incidence of MDA5 autoimmunity and ILD that presented contemporaneously during COVID-19 could
370 be due to an aberrant type 1-centric IFN responses that are shared with autoimmune ILD, but not IPF,
371 which plays out across diverse cell types leading to severe ILD (Figure 6).

372 Our observations, taken together with global reports of similar cases, leads us to propose the
373 term MDA5-autoimmunity and Interstitial Pneumonitis Contemporaneous with the CCOVID-19
374 Pandemic (MIP-C) (Table 2). Such an acronym has credence because of the distinct features that
375 separate MIP-C from the syndrome of MDA5+ DM⁵⁰ including our population being predominantly
376 Caucasian instead of the historically reported MDA5⁺-DM East Asian predilection and the lower rate
377 of ILD that was evident in 42% of cases, at least thus far, to that historically reported in MDA5⁺-DM⁵¹⁻
378 ⁵³. Also the pathogenesis of MDA5⁺-DM is poorly understood but our work in 60 new cases and that
379 from around the world^{2-4,15,18,22,54-67} shows good evidence for a link to SARS-CoV-2 infection and
380 vaccination and possibly both (Figure 2).

381 The MIP-C phenotype, somewhat akin to MIS-C in children, quite often had no history of
382 confirmed SARS-CoV-2 infection. Given that nearly 42% of new cases were not vaccinated prior to
383 MDA5+ disease, it suggests that milder COVID-19 disease, either overt, or covert (i.e., asymptomatic
384 infection or incidental exposure) may be sufficient to cause MDA5 autoimmunity. Given the peak of
385 MDA5 positivity testing followed the peak of COVID-19 cases in 2021, and coincided with the peak of
386 vaccination, these findings suggest an immune reaction or autoimmunity against MDA5 upon SARS-
387 CoV-2 and/or vaccine exposure; it could represent novel immunogenicity in non-immune subjects
388 upon RNA engagement with MDA5, causing a surge of cytokine response, and then the triggering of
389 an autoimmune disease. The development of herd immunity and less respiratory exposure to to SARS-
390 CoV2 could theoretically contribute to the milder phenotype at the population level in our proposed
391 MIP-C entity.

392 As for how COVID-19 vaccine may give rise to such immunogenicity, a recent study by Li et al.,
393 has shed some light⁶⁸. The authors showed that in the lymph nodes (LNs), modified RNA sensed by
394 MDA-5 results in the production of type I interferons (IFNs); the latter induce antigen-specific CD8+ T

395 cell responses ⁶⁸. This conclusion was derived after the authors systematically evaluated the
396 immunogenicity response to BNT162b2 LNP-mRNA against COVID-19 in numerous murine models
397 lacking RNA-sensing pattern recognition receptors [Toll-like receptors 2, 3, 4, 5 and 7 and other
398 inflammasome and necroptosis/pyroptosis pathways] where only MDA-5 was deemed important for
399 type I interferon responses and for antigen-specific CD8⁺ T cell responses ⁶⁸. Because RNA can be
400 recognized by MDA5 in a sequence and structure-dependent manner ⁶⁹, the resultant activation of the
401 innate immune system is believed to be cell, tissue and context specific. Our finding incriminate MDA5
402 protein activation, whether linked to natural infection, or vaccination or potentially both as a trigger
403 for MIP-C and that MDA5-mediated sensing (and mounting of an immunophenotype that is comprised
404 of type 1 interferonopathy and antigen-specific CD8⁺ T cell responses; elaborated below) is a distinct
405 trigger in MIP-C.

406

407 There are four noteworthy findings that inform how we recognize and/or manage MIP-C in
408 the aftermath of COVID-19. First, that the viral sensor *IFIH1*/MDA5 is induced in COVID-19 has been
409 reported exhaustively ^{9,70-77}. We found that the severity of COVID-19 may dictate the risk of
410 progression to ILDs of distinct immunopathogenesis: Milder disease induced *IFIH1* and risk signatures
411 for MDA5-autoimmunity; however, severe disease with diffuse alveolar damage in the setting of acute
412 respiratory distress syndrome (ARDS) induced risk signatures for alveolar dysfunction that are
413 pathognomonic of IPF, consistent with prior claims ³⁰.

414 Second, our finding that the degree of *IFIH1* induction is strongly associated with the degree
415 of induction of a type 1 IFN signature that is quite specific for being IL-15-centric [ViP signature ³⁵] is
416 noteworthy. This finding is in keeping with prior work showing the importance of this IL-15 in rapidly
417 progressing ILD in the setting of MDA5 autoimmunity and amyopathic DM ⁷⁸⁻⁸⁰. Given the extensive
418 literature on the role of the IL15/IL-15RA axis in the development of autoimmunity [reviewed in ⁸¹],
419 and more specifically its role in triggering the activation of CD8⁺ T cells to drive such autoimmunity ⁸²⁻
420 ⁸⁵,

421 Third, the recognition of MIP-C as a syndrome where less than half of cases get severe
422 progressive ILD is relevant for therapy selection including Janus kinase (JAK) inhibitors, such as
423 tofacitinib ⁸⁶ as many cases did not progress, at least in the first two years of MDA5+ status. Fourth,
424 we show that the rs1990760 (p.Ala946Thr) *IFIH1* variant displays, what is likely to be an age-
425 dependent protection ⁷⁴, to a subgroup of patients; these patients show a lesser induction of *IFIH1*, a
426 blunted type 1 IFN storm, and a reduced signature of circulating *ISG15*⁺CD8⁺T cells which was
427 previously found to predict poor one-year survival in MDA5⁺DM patients ⁴².

428 Our study has some limitations, including the retrospective nature of the clinical data collection and
429 uncertainties around the confirmation of COVID19 infection status (most patients were not
430 systematically tested) and could be infected but asymptomatic. Furthermore, we have no data on
431 asymptomatic infection or prolonged carriage status as potential factors in some of these cases;
432 neither did we have patient-derived samples to analyse transcriptomic datasets from our cohort. We
433 also do not delineate how autoimmunity arises; given that MDA5 is a key RNA receptor in the lung
434 parenchymal and immune cells it is tempting to speculate that MDA5 and nucleic acid as an antigen
435 and associated bound adjuvant could contribute to triggering autoimmunity. A clear mechanism for
436 the vascular basis for the DM and PSS lesions is yet to emerge. Regardless, we have shown in numerous
437 independent cohorts that the degree of induction of *IFIH1* (MDA5) is tightly correlated with the degree
438 of induction of type 1 interferons and a gene signature for risk of progressive MDA5+ILD.

439

440 In conclusion, in this work we report a remarkable rise in MDA5+ disease in the Yorkshire region that,
441 given the overall epidemiology, we have termed MIP-C. We provide transcriptome derived insights
442 that point to a plausible and potentially causal link between the surge in anti-MDA5-positivity,
443 autoimmune ILD and COVID-19, but not IPF. These findings warrant further studies, preferably
444 through multi-centre efforts and across nations, to begin to recognize and better appreciate the
445 potential global clinical burden of interstitial pneumonitis and ILD in the aftermath of the COVID-19
446 pandemic.

447 Acknowledgements

448 We thank Guillermo M Albaiceta (Hospital Universitario Central de Asturias, Oviedo, Spain) for access
449 to demographic metadata on published datasets and Debashis Sahoo (UC San Diego) for access to
450 computational tools at the Center for Precision Computational Systems Network (PreCSN). This work
451 was supported in part by the National Institute for Health Research (NIHR) Leeds Biomedical Research
452 Centre (BRC), and in part by the National Institutes for Health (NIH) grant R01-AI155696 and pilot
453 awards from the UC Office of the President (UCOP)-RGPO (R00RG2628, R00RG2642 and R01RG3780)
454 to P.G. S.S was supported in part by R01-AI141630 (to P.G) and in part through funds from the
455 American Association of Immunologists (AAI) Intersect Fellowship Program for Computational
456 Scientists and Immunologists. The views expressed are those of the author(s) and not influenced by
457 the study funders, the NHS, the NIHR or the Department of Health.

458

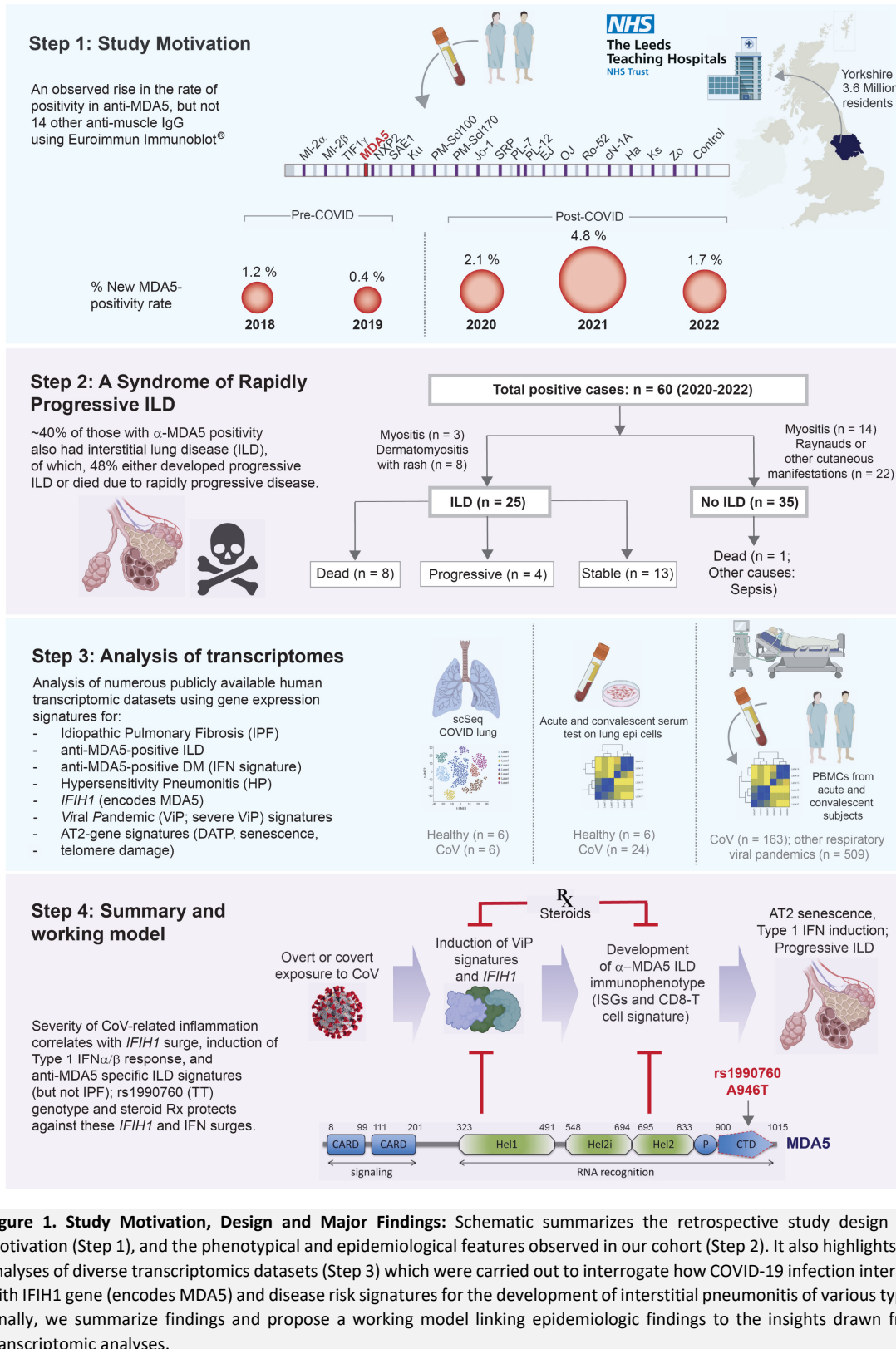
459 Data Availability

460 All data produced in the present work are contained in the manuscript

461

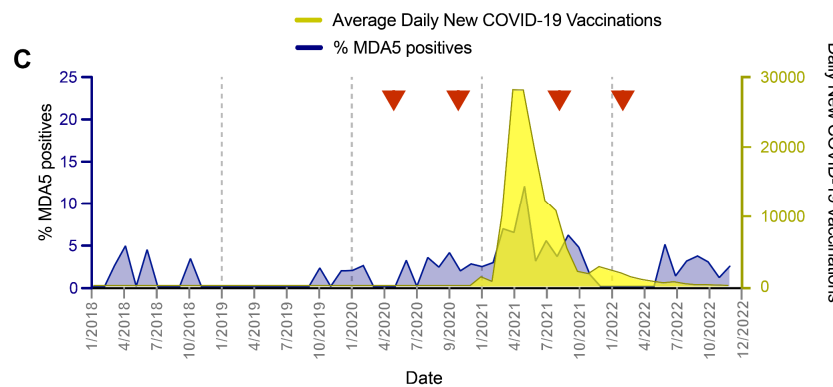
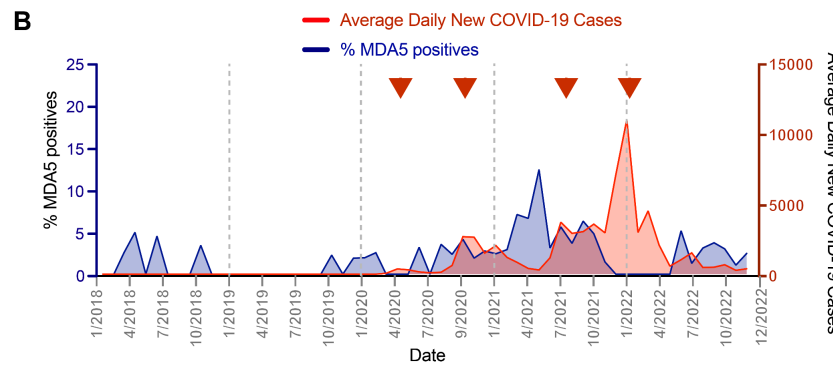
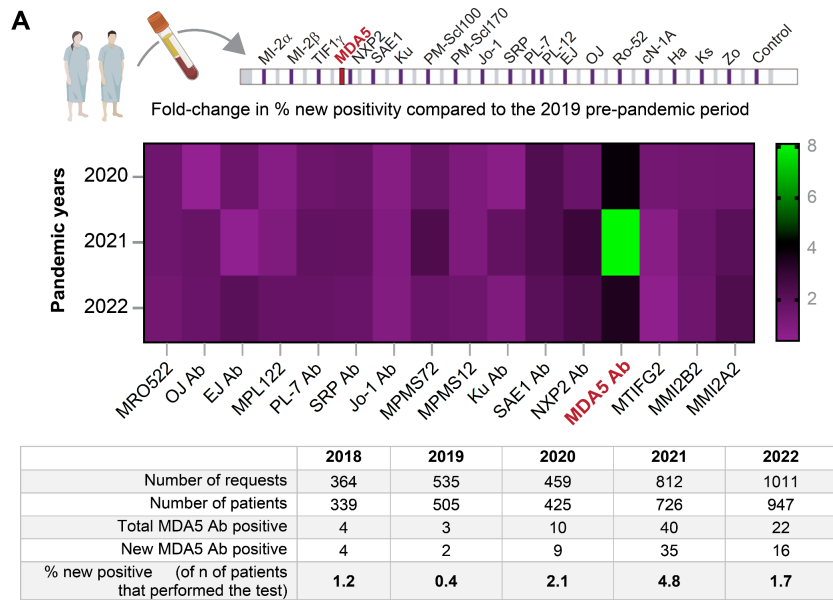
462 Author Contributions

463 SS conducted all the statistical, mathematical, computational, or other formal techniques; ST and EM
464 assisted with dataset processing and curation; KI PD and GDM created all Tables for visualization
465 and data presentation; SS and PG created all figures for visualization and data presentation; DMG
466 conceptualized and supervised all clinical aspects of this study; PG conceptualized and supervised all
467 computational aspects of this study; DM and PG jointly administered the project and secured funding;
468 KI, PD, GDM, DMG and PG wrote initial draft; all authors edited the manuscript and approved its final
469 version.



472

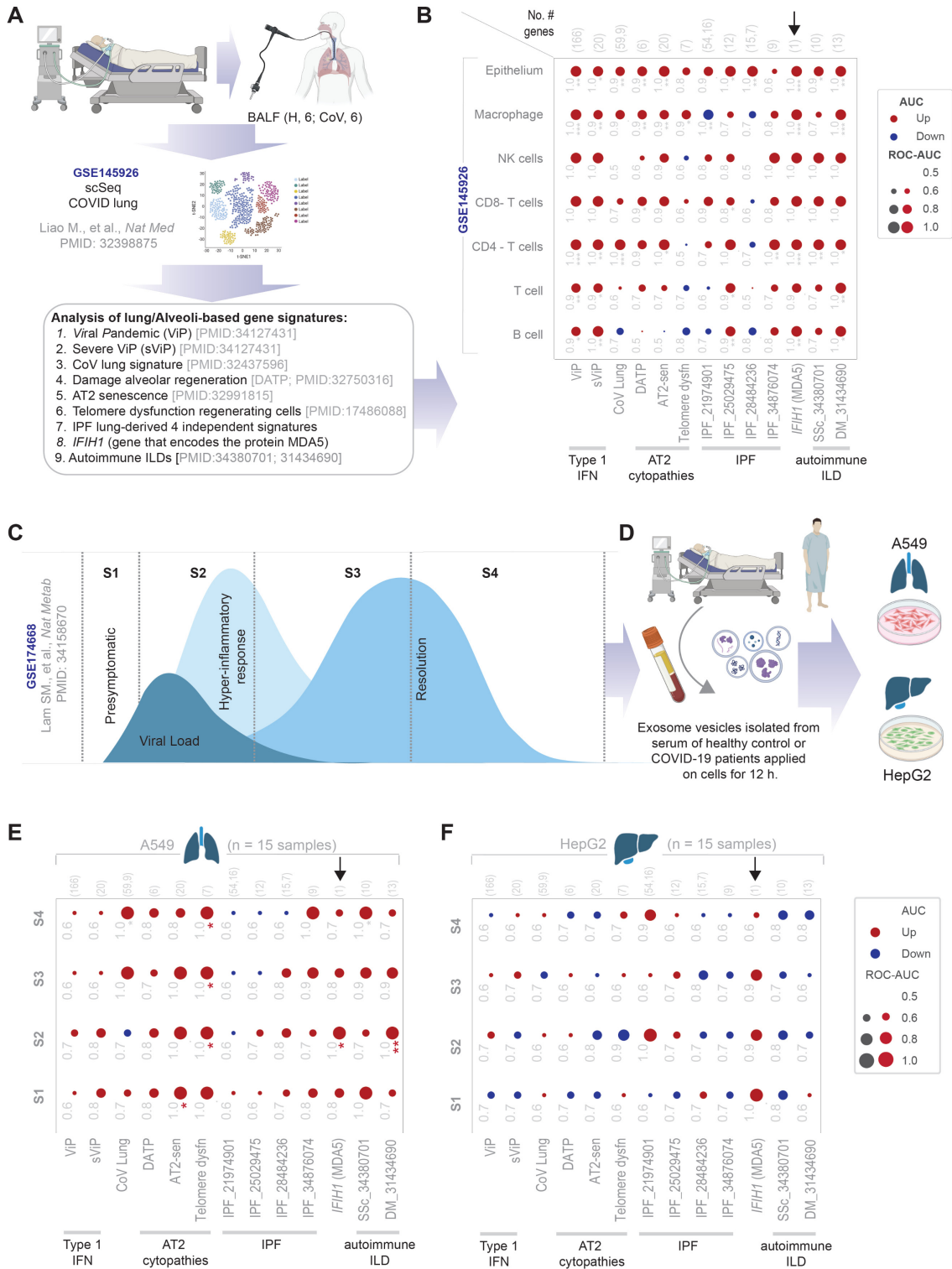
473 **Figure 1. Study Motivation, Design and Major Findings:** Schematic summarizes the retrospective study design and
 474 motivation (Step 1), and the phenotypical and epidemiological features observed in our cohort (Step 2). It also highlights the
 475 analyses of diverse transcriptomics datasets (Step 3) which were carried out to interrogate how COVID-19 infection interacts
 476 with *IFIH1* gene (encodes MDA5) and disease risk signatures for the development of interstitial pneumonitis of various types.
 477 Finally, we summarize findings and propose a working model linking epidemiologic findings to the insights drawn from
 478 transcriptomic analyses.



480

481 **Figure 2 –Rate of MDA5+ testing 2018 to 2022.**

482 **A.** Heatmap (top) shows the fold change in MDA5+ for each of the tested muscle-specific autoantibodies (MSAs),
 483 including anti-MDA5 (using Euroimmun immunoblot®). Table (bottom) provides the actual patient numbers. **B-**
 484 **C.** Graphs display the overlay of newly detected anti-MDA5 positivity (blue; A-B) with either total COVID-19 cases
 485 (red; A) or the rate of new vaccination (yellow; B) that were reported in the Yorkshire and Humber regions since
 486 Jan 2021 to Dec 2022. The COVID-19 case rates and vaccination rates were obtained from the UK.gov database
 487 (<https://coronavirus.data.gov.uk/>). Red arrowheads denote the four waves of COVID-19 cases.



489

490

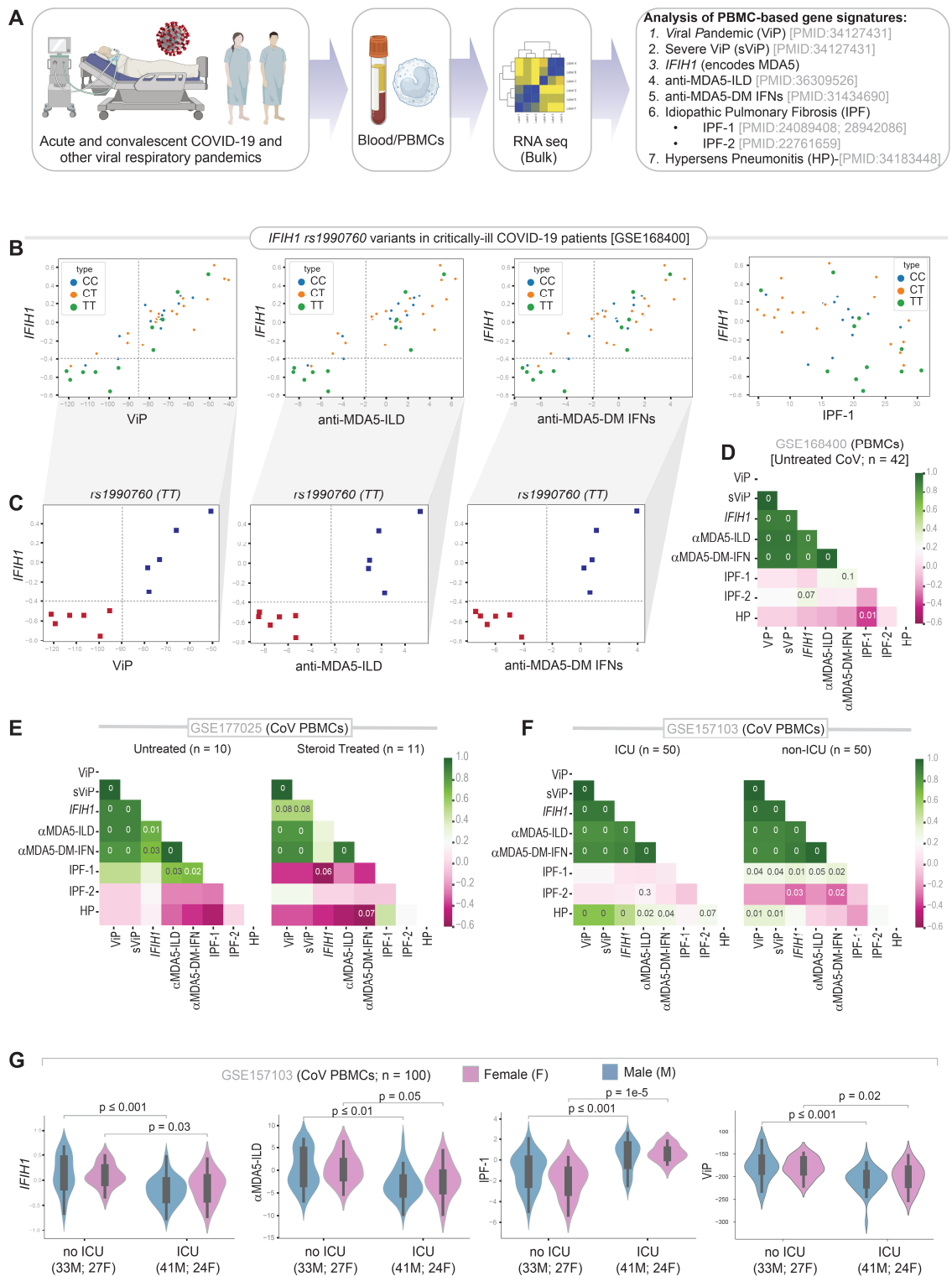
491 **Figure 3. *IFIH1* and autoimmune ILD gene signatures are induced in diverse cell types in CoV lung, including the alveolar**
 492 **epithelium. A.** Schematic showing the study design for panels A-B. **B.** Bubble plot of ROC-AUC values (radii of circles are
 493 **based on the ROC-AUC) demonstrating the direction of gene regulation (Up, red; Down, blue) for the classification of**

494 various cell types between healthy and CoV lung based on various gene signatures in **Fig 3A**, which includes several
495 signatures of AT2 cytopathies that are encountered and implicated in ILD. Numbers indicate PMIDs. Welch's two sample (H
496 vs CoV) unpaired t-test is performed on the composite gene signature score (z-score of normalized tpm count) to compute
497 the *p values* [* . $P \leq 0.05$; ** . $P \leq 0.01$; *** . $P \leq 0.001$]. **C-D**. Schematic summarizes the study design for GSE174668. Panel C
498 shows the natural course of COVID-19 which includes pre-symptomatic (S1), hyperinflammatory (S2), resolution (S3) and
499 convalescent (S4) phases. Typically, S1-2 is SARS-CoV-2 RNA positive and has mixed inflammation and immunosuppression
500 as host immune response to the virus. The second half (S3-4) is characterized by host immune response that is geared
501 towards resolution of inflammation and restoration of homeostasis. Exosome-enriched EVs were isolated from fasting
502 plasma from healthy controls and COVID-19 patients from and then applied on two cell types (Panel D) for 12 h at 37°C
503 prior to RNA Seq analysis.

504 **E-F**: Bubble plot of ROC-AUC values (radii of circles are based on the ROC-AUC) demonstrating the direction of gene
505 regulation (Up, red; Down, blue) for the classification of cells treated with EVs from healthy controls vs those isolated from
506 the indicated phase of CoV infection (S1-4) based on various gene signatures in **Fig 3A**, which includes several signatures of
507 AT2 cytopathies that are encountered and implicated in ILD. Numbers indicate PMIDs. Welch's two sample (H vs CoV)
508 unpaired t-test is performed on the composite gene signature score (z-score of normalized tpm count) to compute the *p*
509 *values* [* . $P \leq 0.05$; ** . $P \leq 0.01$].

510 BALF, bronchoalveolar lavage fluid; H, healthy; CoV, COVID-19; AT2, alveolar type 2 pneumocytes; DATP,
511 damage-associated transient progenitors; SSc, Systemic scleroderma; Sen, senescence.

512



514

515

516

Figure 4. Induction of *IFIH1* in COVID-19 correlates with a Type 1-IFN storm and anti-MDA5-ILD risk signatures in PBMCs.

517

A. Schematic of the workflow in this figure, indicating the types of samples analysed and the gene expression signatures tested.

518

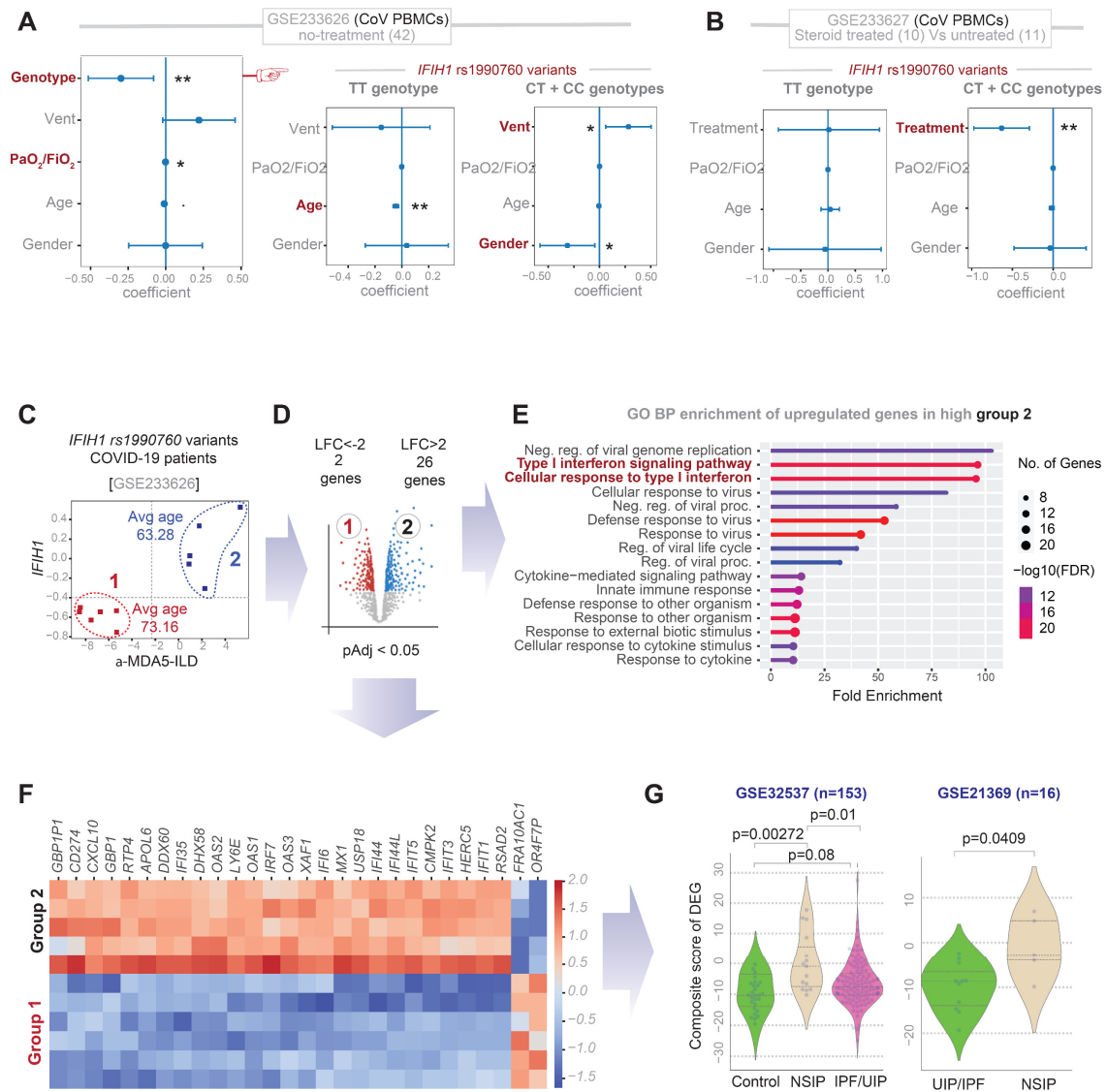
519 **B-C.** Scatter plots show the relationships between *IFIH1* expression (Y axis) and the composite scores of four different
520 gene expression signatures (X axis) in PBMCs from patients with COVID-19. Top panels in B show all three rs1990760
521 variant types. Bottom panels in C show just the TT variant. Interrupted lines are drawn arbitrarily to divide the graph into
522 quadrants with low-low and high-high distributions to separate the patients who suppressed *IFIH1* in the TT genotype from
523 those who did not.

524 **D.** Graphical representation of a correlation matrix representing the correlation between the variables in B-C and
525 additional variables, i.e., composite scores of different gene signatures elaborated in panel A. The colour key spans from -1
526 (magenta) to 1 (green), indicating both strength and direction of correlation. Numbers within the heatmap indicate
527 statistical significance (only significant *p values* are displayed).

528 **E-F.** Correlation matrix showing the correlation between multiple gene signatures (as in D), on two other independent
529 COVID-19 (CoV) patient-derived PBMC datasets. See **Supplementary Figure 2** for similar analyses on three independent
530 PBMC and whole blood datasets representing other respiratory viral pandemics.

531 **G.** Violin plots show the degree of induction of *IFIH1* (transcripts per million; tpm) and various gene expression signature
532 (composite scores) in male or female patients presenting with moderate (non-ICU) or severe (ICU) COVID-19. Welch's two
533 sample (ICU vs non-ICU) unpaired t-test is performed on the tpm (for *IFIH1*) or the composite gene signature score (z-score
534 of normalized tpm count) to compute the *p values* (only significant *p values* are displayed).

535



537

538 **Figure 5. The rs1990760 TT variant of *IFIH1* offers an age-dependent protection against MDA5 surge.**

539 **A-B.** Multivariate analysis of *IFIH1* expression as a linear combination of all variables in the COVID-19 PBMC datasets
 540 GSE233626 (A) and GSE233627 (B). Coefficient of each variable (at the center) with 95% confidence intervals (as error bars)
 541 and the p values were illustrated in the bar plot. The p-value for each term tests the null hypothesis that the coefficient is
 542 equal to zero (no effect). Red = significant co-variates.

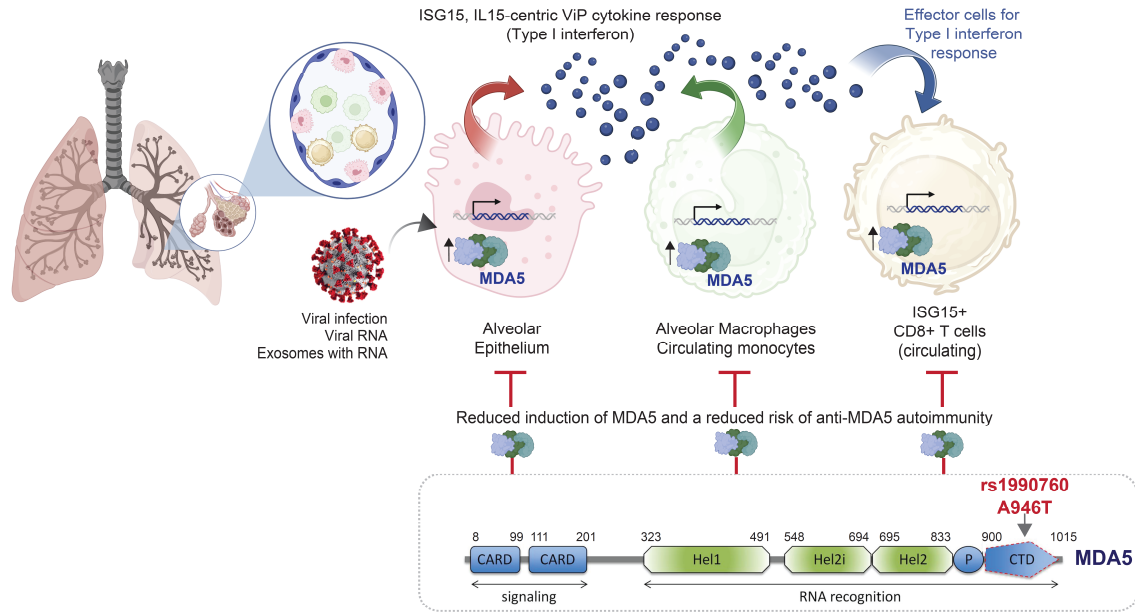
543 **C-E.** Two distinct subgroups of COVID-19 patients with the rs1990760 TT genotype (groups 1 and 2 in the scatter plot in A)
 544 were assessed for differentially expressed genes (DEGs; B). Lollipop graph (C) displays the findings of a gene ontology (GO)
 545 analysis on the list of 26 genes upregulated in group 2.

546 **F.** Heatmap displays DEGs (26 up- and 3 down-regulated; LogFC >2, pAdj 0.05) in group 2 PBMCs compared to group 1.

547 **G.** Violin plots display the composite score of the DEGs (used as a gene signature) in two independent transcriptomic datasets
 548 of lung tissues from subjects with undefined (UIP) or non-specific (NSIP) interstitial pneumonitis and non-diseased controls.

549

550 Figure 6
 551



552

553

554 **Figure 6. Summary and working model.** Schematic summarizes major conclusions and a proposed working model. A type 1-
 555 centric interferon response to the same could serve as pathophysiologic driver of autoimmune ILD involving more than one
 556 cell type. From left to right (*Top*): (i) In the alveolar pneumocytes of COVID-19 lungs, MDA5 is induced and is associated with
 557 type 1 interferon response, AT2 senescence and stem cell dysfunction. MDA5 is induced also in lung epithelial cells upon
 558 exposure to exosome vesicles from patients with acute infection. (ii) In the PBMCs of COVID-19 patients MDA5 is induced in
 559 infected samples, and its degree of induction positively and tightly correlates with an IL-15 centric type 1 interferon response.
 560 (iii) In the PBMCs of COVID-19 patients, there is a concomitant induction of a signature for anti-MDA5 autoimmune ILD
 561 expressed in ISG15+ CD8+ T cells. Bottom panel shows the impact of a protective genotype of the *IFIH1* gene which inhibits
 562 a subset of patients from inducing MDA5 and thereby protects them from a surge of type 1 interferon storm.

563

565 Table 1: MDA5+ Disease split up into ILD and non ILD cases.

	ILD (n=25)	nILD (n=35)
Number of cases, females (%)	12 (48%)	24 (68.6%)
Age in years (mean)	60.28	53.23
Indication for antibody testing		
Dyspnoea (isolated), n (%)	17 (68%)	0 (0%)
Dyspnoea clinically predominant, with associated myositis/dermatomyositis features, n (%)	5 (20%)	0 (0%)
Myositis/dermatomyositis features clinically predominant, with dyspnoea, n (%)	1 (4%)	0 (0%)
Myositis without dermatologic features or dyspnoea, n (%)	0 (0%)	9 (25.7%)
Dermato-myositis-like clinical features, without dyspnoea, n (%)	2 (8%)	10 (28.6%)
Scleroderma-like clinical features, without dyspnoea, n (%)	0 (0%)	8 (22.85%)
Mixed/non-specific clinical features, n (%)	0 (0%)	8 (22.85%)
Autoimmune serology		
ANA IIF positive	15 (60%)	21 (60%)
ANA IIF negative	10 (40%)	14 (40%)
Myositis-associated autoantibodies (n of people with, apart from MDA5)		
Anti-SAE1	7 (28%)	5 (14.3%)
Anti-Ro52	4 (16%)	9 (25.7%)
Anti-PMScl100	2 (8%)	2 (5.7%)
Others	5 (20%)*	13 (37.1%)§
Clinical Features (other than ILD)		
Cutaneous	8 (2%)	10 (28.6%)
Cardiac	0 (0%)	1 (2.9%)
Mechanic's hands	4 (16%)	1 (2.9%)
Synovitis	5 (20%)	15 (39.5%)
Raynaud's phenomenon	3 (12%)	17 (48.6%)
Proximal myopathy	3 (12%)	14 (40%)
Treatment Outcomes		
Response to treatment	5 (20%)**	11 (31.4%)§§

Mortality	8 (32%)	1 (2.85%)§§§
Progressive lung involvement but alive	4 (16%)	0 (0%)
Relationship between MDA5 and COVID-19 Infection/Vaccination		
Infection preceding MDA5 positivity	4 (16%)	4 (11.4%)
Infection after MDA5 positivity	4 (16%)	3 (8.6%)
No known infection	17 (68%)	28 (80%)
Vaccination preceding MDA5 positivity	14 (56%)	22 (62.9%)
Vaccination after MDA5 positivity	6 (24%)	7 (20%)
No vaccination	5 (20%)	6 (17.1%)

MDA5 = Melanoma Differentiation-Associated protein 5; ILD = Interstitial Lung Disease; ANA = Anti-Nuclear Autoantibodies; IIF = Indirect Immuno-fluorescence; COVID-19 = Coronavirus disease 2019 (COVID-19), a contagious disease caused by the Severe Acute Respiratory Syndrome CoronaVirus 2 (SARS-CoV-2).

*some simultaneously with above and between them, anti-PL7 (n=2), anti-SRP (n=2), anti TIF1 (n=1), anti-PL12 (n=1), anti-MI-2-alpha (n=1), anti-PMScl70 (n=1)

**data not available on treatment 1 subjects, 7 were just under observation, with stable disease and 2 died before receiving treatment

§some simultaneously with above and between them, anti-PL7 (n=4), anti-TIF1 (n=1), anti-mi-2-alpha (n=1), anti-mi2-beta (n=1) antiPMScl75 (n=5), anti PScI70 (n=1), anti-NPX2 (n=5), anti-ku (n=4), Anti-TH-to (n=1), anti-RS (n=1), Anti-OJ (n=2), anti-EJ (n=2) and anti-MTIF-gamma 2 (n=2), anti-MPL122 (n=1)

§§6 of patients had no available data regarding treatment, and 12 were at least stable without treatment (on observation), those were not included

§§§ pneumonia infection and sepsis

566
567
568
569
570
571
572
573
574
575
576
577
578
579
580
581

582
583

Table 2 – Comparison between “classic” MDA5+ disease and MIP-C

	Classic MDA5⁺-Disease	MIP-C
Age	Adults 7% MDA5 ⁺ among cases of juvenile dermatomyositis ^{87,88}	4/60 cases (6.6%) children
Gender	Females 66% ⁵⁰	36/60 cases (60%) females
Ethnic background	Asian	32/60 cases (53%) white (British or any other “white” category)*
Lung involvement	Almost universal in people of Asian descent. Pulmonary involvement reported between 39% and 73% elsewhere globally (Brazil, Italy, Spain, North America) ⁵³	25/60 cases (41.6 thus far)
Interstitial lung disease prognosis	Poor, frequently fatal in adults	Fatalities less common, though progressive pulmonary function deterioration frequent (8/60 -13.3%)
Isolated, Non-Pulmonary Disease	Uncommon	35/60 cases (58.3%) experienced manifestations of connective tissue diseases (18/60 cutaneous rash; 20/60 Raynaud’s phenomenon; 5/60 “mechanic’s hands”, some of the 35 have more than one combined)
Associated antibody positivity		About two third cases have associated antibody positivity (36/60), being anti Ro 52 (13/60) and Anti SAE1 (12/60) the most common.

584 In the Yorkshire region of UK, the estimate for population classified as “white” (any “white”
585 category) was 85.4%, according to 2021 UK census. Such percentage reflects the difference in
586 prevalence recorded for the whole England and Wales population (81.7%) at the time of 2021 UK
587 census. *14/60 patients had no ethnicity available.

588

665 References

- 666 1. Astorri D, Nalotto L, Vaccaro E, et al. AB0715 Anti-MDA5 Dermatomyositis after BNT162b2
667 vaccination. *Ann Rheum Dis* 2022; **81**(Suppl 1): 1484.
- 668 2. Gonzalez D, Gupta L, Murthy V, et al. Anti-MDA5 dermatomyositis after COVID-19
669 vaccination: a case-based review. *Rheumatol Int* 2022; **42**(9): 1629-41.
- 670 3. Kitajima T, Funauchi A, Nakajima T, Marumo S, Imura Y, Fukui M. Antimelanoma
671 Differentiation-Associated Gene 5 Antibody-Positive Interstitial Lung Disease After Vaccination With
672 COVID-19 mRNA Vaccines. (0315-162X (Print)).
- 673 4. Sugimoto TA-O, Yorishima A, Oka N, et al. Appearance of anti-MDA5 antibody-positive
674 dermatomyositis after COVID-19 vaccination. (2472-5625 (Electronic)).
- 675 5. Nakashima R, Imura Y, Kobayashi S, et al. The RIG-I-like receptor IFIH1/MDA5 is a
676 dermatomyositis-specific autoantigen identified by the anti-CADM-140 antibody. *Rheumatology*
677 (*Oxford*) 2010; **49**(3): 433-40.
- 678 6. Fiorentino D, Chung L, Zwerner J, Rosen A, Casciola-Rosen L. The mucocutaneous and
679 systemic phenotype of dermatomyositis patients with antibodies to MDA5 (CADM-140): a
680 retrospective study. *J Am Acad Dermatol* 2011; **65**(1): 25-34.
- 681 7. Sato S, Hoshino K, Satoh T, et al. RNA helicase encoded by melanoma differentiation-
682 associated gene 5 is a major autoantigen in patients with clinically amyopathic dermatomyositis:
683 Association with rapidly progressive interstitial lung disease. *Arthritis Rheum* 2009; **60**(7): 2193-200.
- 684 8. Yamada T, Sato S, Sotoyama Y, et al. RIG-I triggers a signaling-abortive anti-SARS-CoV-2
685 defense in human lung cells. *Nat Immunol* 2021; **22**(7): 820-8.
- 686 9. Amado-Rodriguez L, Salgado Del Riego E, Gomez de Ona J, et al. Effects of IFIH1 rs1990760
687 variants on systemic inflammation and outcome in critically ill COVID-19 patients in an observational
688 translational study. *Elife* 2022; **11**.
- 689 10. Wang G, Wang Q, Wang YM, et al. Presence of Anti-MDA5 Antibody and Its Value for the
690 Clinical Assessment in Patients With COVID-19: A Retrospective Cohort Study. *Front Immunol* 2021;
691 **12**.
- 692 11. Swartzman I, Gu JJ, Toner Z, Grover R, Suresh L, Ullman LE. Prevalence of Myositis-Specific
693 Autoantibodies and Myositis-Associated Autoantibodies in COVID-19 Patients: A Pilot Study and
694 Literature Review. *Cureus* 2022; **14**(9): e29752.
- 695 12. Aschman T, Schneider J, Greuel S, et al. Association Between SARS-CoV-2 Infection and
696 Immune-Mediated Myopathy in Patients Who Have Died. *Jama Neurol* 2021; **78**(8): 948-60.
- 697 13. Anderle K, Machold K, Kiener HP, et al. COVID-19 as a putative trigger of anti-MDA5-
698 associated dermatomyositis with acute respiratory distress syndrome (ARDS) requiring lung
699 transplantation, a case report. *Bmc Rheumatol* 2022; **6**(1).
- 700 14. Changzheng L, Qian W, Yeming W, et al. Analysis of the correlation between anti-MDA5
701 antibody and the severity of COVID-19: a retrospective study. *medRxiv* 2020: 2020.07.29.20164780.
- 702 15. Wang SA-O, Noumi B, Malik FA-O, Wang SA-O. A Rare Case of MDA-5-Positive Amyopathic
703 Dermatomyositis with Rapidly Progressive Interstitial Lung Disease Following COVID-19 mRNA
704 Vaccination - a Case Report. (2523-8973 (Electronic)).
- 705 16. Maezawa Y, Narita M, Tanimura R, Hattori S, Satoh H. Rapidly Progressive Interstitial Lung
706 Disease Associated with Melanoma Differentiation-Associated Gene 5 Antibody. (1805-9694
707 (Electronic)).
- 708 17. Wang YA-O, Du G, Zhang GA-O, Matucci-Cerinic M, Furst DE. Similarities and differences
709 between severe COVID-19 pneumonia and anti-MDA-5-positive dermatomyositis-associated rapidly
710 progressive interstitial lung diseases: a challenge for the future. (1468-2060 (Electronic)).
- 711 18. Takahashi SA-O, Kato A, Hashimoto K, Takehara T, Ishioka KA-O, Takanashi S. A case of anti-
712 melanoma differentiation-associated gene 5 antibody-positive dermatomyositis-associated rapidly
713 progressive interstitial lung diseases developed after administration of COVID-19 vaccine and
714 subsequent pneumococcal vaccine. (2051-3380 (Print)).

- 715 19. Teo KF, Chen DY, Hsu JT, et al. Screening and characterization of myositis-related
716 autoantibodies in COVID-19 patients. (1752-8062 (Electronic)).
- 717 20. Cao Y, Zhou J, Cao T, Zhang G, Pan HA-O. Management of dermatomyositis patients amidst
718 the COVID-19 pandemic: Two case reports. (1536-5964 (Electronic)).
- 719 21. Bobirca AA-O, Alexandru CA-O, Musetescu AE, et al. Anti-MDA5 Amyopathic
720 Dermatomyositis-A Diagnostic and Therapeutic Challenge. LID - 10.3390/life12081108 [doi] LID -
721 1108. (2075-1729 (Print)).
- 722 22. García-Bravo L, Calle-Rubio M, Fernández-Arquero M, et al. Association of anti-SARS-COV-2
723 vaccine with increased incidence of myositis-related anti-RNA-synthetases auto-antibodies. (2589-
724 9090 (Electronic)).
- 725 23. Mecoli CA-O, Yoshida A, Paik JA-O, et al. Presence and Implications of Anti-Angiotensin
726 Converting Enzyme-2 Immunoglobulin M Antibodies in Anti-Melanoma-Differentiation-Associated 5
727 Dermatomyositis. (2578-5745 (Electronic)).
- 728 24. Gupta P, Kharbanda R, Lawrence A, Gupta L. Systemic flare and cutaneous ulceration
729 following cytomegalovirus infection in a patient with anti-melanoma differentiation-associated
730 protein 5 (MDA5) associated myositis: Diagnostic challenge during the time of coronavirus disease
731 (COVID-19) pandemic. (2090-2433 (Electronic)).
- 732 25. De Santis M, Isailovic N, Motta F, et al. Environmental triggers for connective tissue disease:
733 the case of COVID-19 associated with dermatomyositis-specific autoantibodies. (1531-6963
734 (Electronic)).
- 735 26. Kondo Y, Kaneko Y, Takei H, et al. COVID-19 shares clinical features with anti-melanoma
736 differentiation-associated protein 5 positive dermatomyositis and adult Still's disease. (0392-856X
737 (Print)).
- 738 27. Quintana-Ortega CA-O, Remesal A, Ruiz de Valbuena M, et al. Fatal outcome of anti-MDA5
739 juvenile dermatomyositis in a paediatric COVID-19 patient: a case report. (2472-5625 (Electronic)).
- 740 28. Gono T, Sato S Fau - Kawaguchi Y, Kawaguchi Y Fau - Kuwana M, et al. Anti-MDA5 antibody,
741 ferritin and IL-18 are useful for the evaluation of response to treatment in interstitial lung disease
742 with anti-MDA5 antibody-positive dermatomyositis. (1462-0332 (Electronic)).
- 743 29. <https://digital.nhs.uk/services/spine>. (accessed October, 7 2023).
- 744 30. Sinha S, Castillo V, Espinoza CR, et al. COVID-19 lung disease shares driver AT2 cytopathic
745 features with Idiopathic pulmonary fibrosis. (2352-3964 (Electronic)).
- 746 31. Noble PW, Barkauskas CE, Jiang D. Pulmonary fibrosis: patterns and perpetrators. *J Clin*
747 *Invest* 2012; **122**(8): 2756-62.
- 748 32. Sahoo D, Dill DL, Tibshirani R, Plevritis SK. Extracting binary signals from microarray time-
749 course data. *Nucleic Acids Res* 2007; **35**(11): 3705-12.
- 750 33. Sinha S, Castillo V, Espinoza CR, et al. COVID-19 lung disease shares driver AT2 cytopathic
751 features with Idiopathic pulmonary fibrosis. *EBioMedicine* 2022; **82**: 104185.
- 752 34. Statistics OfN. National identity, ethnic group, language and religion question development
753 for Census 2021.
- 754 35. Sahoo D, Katkar GD, Khandelwal S, et al. AI-guided discovery of the invariant host response
755 to viral pandemics. *Ebiomedicine* 2021; **68**.
- 756 36. Ackermann M, Verleden SE, Kuehnel M, et al. Pulmonary Vascular Endothelialitis,
757 Thrombosis, and Angiogenesis in Covid-19. *New Engl J Med* 2020; **383**(2): 120-8.
- 758 37. Choi J, Park JE, Tsagkogeorga G, et al. Inflammatory Signals Induce AT2 Cell-Derived Damage-
759 Associated Transient Progenitors that Mediate Alveolar Regeneration. *Cell Stem Cell* 2020; **27**(3):
760 366-+.
- 761 38. Kobayashi Y, Tata A, Konkimalla A, et al. Persistence of a regeneration-associated,
762 transitional alveolar epithelial cell state in pulmonary fibrosis. *Nat Cell Biol* 2020; **22**(8): 934-+.
- 763 39. Strunz M, Simon LM, Ansari M, et al. Alveolar regeneration through a Krt8+transitional stem
764 cell state that persists in human lung fibrosis. *Nat Commun* 2020; **11**(1).

- 765 40. Yao CF, Guan XR, Carraro G, et al. Senescence of Alveolar Type 2 Cells Drives Progressive
766 Pulmonary Fibrosis. *Am J Resp Crit Care* 2021; **203**(6): 707-17.
- 767 41. Ju ZY, Jiang H, Jaworski M, et al. Telomere dysfunction induces environmental alterations
768 limiting hematopoietic stem cell function and engraftment. *Nat Med* 2007; **13**(6): 742-7.
- 769 42. Ye Y, Chen Z, Jiang S, et al. Single-cell profiling reveals distinct adaptive immune hallmarks in
770 MDA5+ dermatomyositis with therapeutic implications. *Nat Commun* 2022; **13**(1): 6458.
- 771 43. Herazo-Maya JD, Noth I, Duncan SR, et al. Peripheral blood mononuclear cell gene
772 expression profiles predict poor outcome in idiopathic pulmonary fibrosis. *Sci Transl Med* 2013;
773 **5**(205): 205ra136.
- 774 44. Herazo-Maya JD, Sun JH, Molyneaux PL, et al. Validation of a 52-gene risk profile for
775 outcome prediction in patients with idiopathic pulmonary fibrosis: an international, multicentre,
776 cohort study. *Lancet Resp Med* 2017; **5**(11): 857-68.
- 777 45. Kameda M, Otsuka M, Chiba H, Kuronuma K, Hasegawa T, Takahashi H. CXCL9, CXCL10, and
778 CXCL11; biomarkers of pulmonary inflammation associated with autoimmunity in patients with
779 collagen vascular diseases-associated interstitial lung disease and interstitial pneumonia with
780 autoimmune features. *Plos One* 2020; **15**(11).
- 781 46. Baglaenko Y, Chang NH, Johnson SR, et al. The presence of anti-nuclear antibodies alone is
782 associated with changes in B cell activation and T follicular helper cells similar to those in systemic
783 autoimmune rheumatic disease. *Arthritis Res Ther* 2018; **20**.
- 784 47. Hamano Y, Kida H, Ihara S, et al. Classification of idiopathic interstitial pneumonias using
785 anti-myxovirus resistance-protein 1 autoantibody. *Sci Rep-Uk* 2017; **7**.
- 786 48. Wang H, Chen X, Du Y, et al. Mortality risk in patients with anti-MDA5 dermatomyositis is
787 related to rapidly progressive interstitial lung disease and anti-Ro52 antibody. *Arthritis Res Ther*
788 **2023**; **25**(1): 127.
- 789 49. So J, So H, Wong VT, et al. Predictors of rapidly progressive interstitial lung disease and
790 mortality in patients with autoantibodies against melanoma differentiation-associated protein 5
791 dermatomyositis. *Rheumatology (Oxford)* 2022; **61**(11): 4437-44.
- 792 50. Wu W, Guo L, Fu Y, et al. Interstitial Lung Disease in Anti-MDA5 Positive Dermatomyositis.
793 *Clin Rev Allergy Immunol* 2021; **60**(2): 293-304.
- 794 51. Narang NS, Casciola-Rosen L, Li S, Chung L, Fiorentino DF. Cutaneous ulceration in
795 dermatomyositis: association with anti-melanoma differentiation-associated gene 5 antibodies and
796 interstitial lung disease. *Arthritis Care Res (Hoboken)* 2015; **67**(5): 667-72.
- 797 52. Sato S, Hirakata M, Kuwana M, et al. Autoantibodies to a 140-kd polypeptide, CADM-140, in
798 Japanese patients with clinically amyopathic dermatomyositis. *Arthritis Rheum* 2005; **52**(5): 1571-6.
- 799 53. Nombel A, Fabien N, Coutant F. Dermatomyositis With Anti-MDA5 Antibodies: Bioclinical
800 Features, Pathogenesis and Emerging Therapies. *Front Immunol* 2021; **12**: 773352.
- 801 54. De Marco G, Giryes S, Williams K, et al. A Large Cluster of New Onset Autoimmune Myositis
802 in the Yorkshire Region Following SARS-CoV-2 Vaccination. *Vaccines (Basel)* 2022; **10**(8).
- 803 55. Camargo-Coronel A, Quinones-Moya H, Hernandez-Zavala MR, Hernandez-Vazquez JR,
804 Vazquez-Zaragoza MA. Idiopathic inflammatory myopathies linked to vaccination against SARS-CoV-
805 2: a systematic review. *Reumatismo* 2023; **75**(1).
- 806 56. Syrmou V, Liaskos C, Ntavari N, et al. COVID-19 vaccine-associated myositis: a
807 comprehensive review of the literature driven by a case report. *Immunol Res* 2023: 1-10.
- 808 57. Rimmer S, Ly L, Boh E. Subacute cutaneous lupus erythematosus after mRNA-based SARS-
809 CoV-2 vaccination. *JAAD Case Rep* 2023; **33**: 70-2.
- 810 58. Chan AR, Cohen Tervaert JW, Redmond D, et al. A case series of dermatomyositis following
811 SARS-CoV-2 vaccination. *Front Med (Lausanne)* 2022; **9**: 1013378.
- 812 59. Ding Y, Ge Y. Inflammatory myopathy following coronavirus disease 2019 vaccination: A
813 systematic review. *Front Public Health* 2022; **10**: 1007637.
- 814 60. Yang L, Ye T, Liu H, Huang C, Tian W, Cai Y. A case of Anti-MDA5-Positive dermatomyositis
815 after inactivated COVID-19 vaccine. *J Eur Acad Dermatol Venereol* 2023; **37**(2): e127-e9.

- 816 61. Holzer MT, Krusche M, Ruffer N, et al. New-onset dermatomyositis following SARS-CoV-2
817 infection and vaccination: a case-based review. *Rheumatol Int* 2022; **42**(12): 2267-76.
- 818 62. Chaima K, Mariem A, Sana B, et al. Vaccine-induced dermatomyositis following COVID-19
819 vaccination. *Dermatol Ther* 2022; **35**(10): e15749.
- 820 63. Gil-Vila A, Ravichandran N, Selva-O'Callaghan A, et al. COVID-19 Vaccination in Autoimmune
821 Diseases (COVAD) study: Vaccine safety in idiopathic inflammatory myopathies. *Muscle Nerve* 2022;
822 **66**(4): 426-37.
- 823 64. Gouda W, Albasri A, Alsaqabi F, Al Sabah HY, Alkandari M, Abdelnaby H. Dermatomyositis
824 Following BNT162b2 mRNA COVID-19 Vaccination. *J Korean Med Sci* 2022; **37**(5): e32.
- 825 65. Hinterseher J, Hertl M, Didona D. Autoimmune skin disorders and SARS-CoV-2 vaccination - a
826 meta-analysis. *J Dtsch Dermatol Ges* 2023.
- 827 66. Lee AYS, Lee C, Brown DA, Suan D. Development of anti-NXP2 dermatomyositis following
828 Comirnaty COVID-19 vaccination. *Postgrad Med J* 2023; **99**(1170): 363-4.
- 829 67. Tada T, Murao H, Shiratani R, et al. Spontaneous resolution of inflammatory myopathy
830 involving the masseter muscle following COVID-19 mRNA vaccination. *Mod Rheumatol Case Rep*
831 2023.
- 832 68. Li C, Lee A, Grigoryan L, et al. Mechanisms of innate and adaptive immunity to the Pfizer-
833 BioNTech BNT162b2 vaccine. *Nat Immunol* 2022; **23**(4): 543-55.
- 834 69. de Oliveira Mann CC, Hornung V. Molecular mechanisms of nonself nucleic acid recognition
835 by the innate immune system. *Eur J Immunol* 2021; **51**(8): 1897-910.
- 836 70. Thorne LG, Reuschl AK, Zuliani-Alvarez L, et al. SARS-CoV-2 sensing by RIG-I and MDA5 links
837 epithelial infection to macrophage inflammation. *Embo J* 2021; **40**(15): e107826.
- 838 71. Liu G, Lee JH, Parker ZM, et al. ISG15-dependent activation of the sensor MDA5 is
839 antagonized by the SARS-CoV-2 papain-like protease to evade host innate immunity. *Nat Microbiol*
840 2021; **6**(4): 467-78.
- 841 72. Han L, Zhuang MW, Deng J, et al. SARS-CoV-2 ORF9b antagonizes type I and III interferons by
842 targeting multiple components of the RIG-I/MDA-5-MAVS, TLR3-TRIF, and cGAS-STING signaling
843 pathways. *J Med Virol* 2021; **93**(9): 5376-89.
- 844 73. Yin X, Riva L, Pu Y, et al. MDA5 Governs the Innate Immune Response to SARS-CoV-2 in Lung
845 Epithelial Cells. *Cell Rep* 2021; **34**(2): 108628.
- 846 74. Muñoz-Banciella MG, Albaiceta GM, Amado-Rodríguez L, et al. Age-dependent effect of the
847 IFIH1/MDA5 gene variants on the risk of critical COVID-19. (1432-1211 (Electronic)).
- 848 75. Sampaio NG, Chauveau L, Hertzog J, et al. The RNA sensor MDA5 detects SARS-CoV-2
849 infection. *Sci Rep* 2021; **11**(1): 13638.
- 850 76. Russ A, Wittmann S, Tsukamoto Y, et al. Nsp16 shields SARS-CoV-2 from efficient MDA5
851 sensing and IFIT1-mediated restriction. *EMBO Rep* 2022; **23**(12): e55648.
- 852 77. Rebendenne A, Valadão ALC, Tauziet M, et al. SARS-CoV-2 triggers an MDA-5-dependent
853 interferon response which is unable to control replication in lung epithelial cells. *J Virol* 2021; **95**(8).
- 854 78. Takada T, Ohashi K, Hayashi M, et al. Role of IL-15 in interstitial lung diseases in amyopathic
855 dermatomyositis with anti-MDA-5 antibody. *Respiratory Medicine* 2018; **141**: 7-13.
- 856 79. Shimizu T, Koga T, Furukawa K, et al. IL-15 is a biomarker involved in the development of
857 rapidly progressive interstitial lung disease complicated with polymyositis/dermatomyositis. *Journal*
858 *of Internal Medicine* 2021; **289**(2): 206-20.
- 859 80. Hu H, Yang H, Liu Y, Yan B. Pathogenesis of Anti-melanoma Differentiation-Associated Gene
860 5 Antibody-Positive Dermatomyositis: A Concise Review With an Emphasis on Type I Interferon
861 System. *Front Med-Lausanne* 2022; **8**.
- 862 81. Allard-Chamard H, Mishra HK, Nandi M, et al. Interleukin-15 in autoimmunity. *Cytokine*
863 2020; **136**: 155258.
- 864 82. Li J, Zaslavsky M, Su Y, et al. KIR+CD8+ T cells suppress pathogenic T cells and are active in
865 autoimmune diseases and COVID-19. *Science*; **376**(6590): eabi9591.

866 83. Watkinson F, Nayar SK, Rani A, et al. IL-15 Upregulates Telomerase Expression and Potently
867 Increases Proliferative Capacity of NK, NKT-Like, and CD8 T Cells. *Front Immunol* 2021; **11**.
868 84. Anthony SM, Schluns KS. Emerging roles for IL-15 in the activation and function of T-cells
869 during immune stimulation. *Res Rep Biol* 2015; **6**: 25-37.
870 85. Collier JL, Weiss SA, Pauken KE, Sen DR, Sharpe AH. Not-so-opposite ends of the spectrum:
871 CD8+ T cell dysfunction across chronic infection, cancer and autoimmunity. *Nat Immunol* 2021;
872 **22**(7): 809-19.
873 86. Selva-O'Callaghan AA-O, Romero-Bueno F, Trallero-Araguás E, et al. Pharmacologic
874 Treatment of Anti-MDA5 Rapidly Progressive Interstitial Lung Disease. (2198-6002 (Print)).
875 87. Tansley SL, Betteridge ZE, Gunawardena H, et al. Anti-MDA5 autoantibodies in juvenile
876 dermatomyositis identify a distinct clinical phenotype: a prospective cohort study. *Arthritis Res Ther*
877 2014; **16**(4): R138.
878 88. Mamyrova G, Kishi T, Shi M, et al. Anti-MDA5 autoantibodies associated with juvenile
879 dermatomyositis constitute a distinct phenotype in North America. *Rheumatology (Oxford)* 2021;
880 **60**(4): 1839-49.

881